High-resolution CFD simulations of forced convective heat transfer coefficients at exterior building surfaces

Bert Blocken, PhD, MASc
Eindhoven University of Technology, The Netherlands
b.j.e.blocken@tue.nl

Thijs Defraeye, MASc
Katholieke Universiteit Leuven, Belgium

Adam Neale, MASc
Concordia University, Montreal, Canada

Dominique Derome, Prof, PhD, MASc
Empa, Swiss Federal Laboratories for Materials Testing and Research, Switzerland

Jan Carmeliet, Prof, PhD, MASc
Chair of Building Physics, Swiss Federal Institute of Technology ETHZ, Zürich, Switzerland;
Empa, Swiss Federal Laboratories for Materials Testing and Research, Switzerland

KEYWORDS: *wind flow; Computational Fluid Dynamics; boundary layer; heat and mass transfer*

SUMMARY:
High-resolution CFD simulations of forced convective heat transfer at the facades of a low-rise cubic building (10x10x10m³) are conducted to determine convective heat transfer coefficients (CHTC). CFD model validation is performed based on wind tunnel measurements of the upstream near-field velocity pattern. A particular feature of the CFD simulations is the use of a high-resolution grid with control volumes of only 160 μm near the building surfaces to resolve the entire boundary layer, including the laminar sublayer that dominates the convective surface resistance. The study shows that: (1) wind flow around the building introduces a very distinct CHTC distribution across the facade; (2) no significant correlation exists between the CHTC and the local wind speed across the facade; (3) for a reference wind speed of 3 m/s, the laminar sublayer has a thickness of about 1 mm; (4) standard and non-equilibrium wall functions are not able to capture the complexity of wind-induced heat transfer, therefore low-Reynolds number modelling on high-resolution grids is imperative; (5) the CHTC distribution across the windward facade shows some similarity to the distribution of wind-driven rain (WDR), with both parameters reaching high levels near the top edge of the facade. This suggests that also the convective vapour transfer coefficient will be higher at this location and that the facade parts that receive most WDR also experience most intensive drying.

1. Introduction

Hygrothermal (HAM) analysis of building components requires the knowledge of the convective heat (h_c) and vapour (β) transfer coefficients at exterior and interior building surfaces:

$$q_c = h_c(T_{ref} - T_s); \qquad g_v = \beta(p_{v,ref} - p_{v,s}) \tag{1-2}$$

where q_c is the convective heat flux density (W/m²), h_c the CHTC (W/m²K), T_c the reference temperature (K) and T_S the surface temperature (K). g_v is the vapour flux density (kg/m²s), β the convective vapour transfer coefficient (CVTC) (s/m), $p_{v,ref}$ the reference vapour pressure (Pa) and $p_{v,s}$ the vapour pressure at the surface (Pa). Most research on CHTC and CVTC in the past has focused on interior conditions. Exterior transfer coefficients have received relatively little attention. Exterior transfer coefficients are a complex function of building geometry, local wind speed, turbulence intensity, surface roughness, texture and geometry, temperature, moisture content, etc. Little however is known about the actual values and the variability of these coefficients across building facades as a function of the different parameters.

This paper focuses on exterior CHTC only. In the past, three methods have been employed to investigate and determine exterior CHTC: wind tunnel measurements, full-scale measurements and numerical simulations based

on Computational Fluid Dynamics (CFD). By far most research has been experimental. Only more recently, CFD has been introduced in this field.

Jürges (1924) performed a wind tunnel study of the convective heat transfer from small, flat, heated plates attached to the wall of the wind tunnel. He provided the following relationship of h_c with the free-stream wind speed in the tunnel V_∞:

$$h_c = 4.0V_\infty + 5.6 \;\; ; \;\; V_\infty < 5\ m/s; \qquad h_c = 7.1V_\infty^{0.78} + 5.6 \;\; ; \;\; V_\infty > 5\ m/s \tag{3-4}$$

These results were the basis of the design values of h_c given in the CIBS Guide (1979). Although the influence of wind speed is very important, as indicated by Eqs. (3,4), this Guide does not provide sufficient information on local wind speed. Actually, V_∞ in Eqs. (3,4) has been replaced by the local wind speed $V_{3D,loc}$, although both parameters can be considerably different. Furthermore, the Guide assumes a constant value of $V_{3D,loc}$ across the facade and does not specify at what distance from the facade this value has to be taken. Note that the subscript 3D refers to the magnitude of the 3D velocity vector.

From the mid 1960's, several attempts were made to measure h_c with heated plates or strips on full-scale buildings. Detailed work was done by Ito et al. (1972) who measured h_c, $V_{3D,loc}$ (at 0.3 m distance from the heated surface) and $V_{3D,R}$ (roof-top wind speed) at the facade of a 6-storey building in Tokyo. Two important conclusions from this work were: (1) The h_c-$V_{3D,loc}$ relationship is relatively independent of surface location and wind direction; and (2) $V_{3D,loc}$ is about 0.20-0.33 times $V_{3D,R}$. These conclusions however can be questioned, since the results were obtained from only a few measurement positions on the facade and for a narrow range of wind directions. The work by Ito et al. (1972) was the basis for the empirical relationships between $V_{3D,S}$, U_{10} and h_c set forth by ASHRAE (1975). Surprisingly and unfortunately, $V_{3D,R}$ in the equations of Ito et al. (1972) appears to have been substituted by U_{10}, while it has been often shown in wind engineering studies that the difference between U_{10} and $V_{3D,R}$ can be very large. Sharples (1984) measured h_c, $V_{3D,loc}$ (at 1 m from the surface) and $V_{3D,R}$ for a high-rise building, as well as U_{10} at a nearby meteorological station. As opposed to the findings by Ito et al. (1972), the h_c-$V_{3D,loc}$ relationship did not appear to be independent of surface location and wind direction. Sharples attributed this to the limited number of measurement points in the study by Ito et al. (1972) and to the specific features of the boundary layer near the building edges. The disadvantage however of the work by Sharples (1984) is the rough classification of wind direction (only two classes: windward and leeward): "data was classified as windward if the angle of incidence between the normal to the monitored facade and the wind direction was less than +/-90° and leeward for all other directions". Since the wind-flow pattern around a building changes markedly with wind direction, this is considered to be one of the main reasons for the low correlation coefficients found by Sharples (1984). For a "worst-case" situation, i.e. a location at the top edge of a 18-storey high-rise building, Sharples (1984) presents the following relationship:

$$h_c = 1.7V_{3D,loc} + 5.1 \tag{5}$$

where $V_{3D,loc}$ is the local wind speed (m/s) measured at 1 m distance from the surface. It is expressed as a simple function of the reference wind speed U_{10}:

$$V_{3D,loc} = 1.8U_{10} + 0.2 \;\; (windward); \qquad V_{3D,loc} = 0.4U_{10} + 1.7 \;\; (leeward) \tag{6-7}$$

CFD simulations of the forced exterior CHTC on the surfaces of a rectangular building model were performed by Emmel et al. (2007). However, the low resolution of the grid near the building surfaces and the use of wall functions have compromised the accuracy of the calculated CHTC, as will be shown later in the present paper.

It is known that exterior CHTC are to a large extent influenced by the local wind speed near the surface ($V_{3D,loc}$) and that the relationship CHTC-$V_{3D,loc}$ is dependent on the building geometry and the position on the building facade. Many HAM models use the equations by Sharples (1984) for CHTC, and the convective vapour transfer coefficients are generally determined from the CHTC using the Chilton-Colburn analogy that assumes conformity between the thermal and hygric boundary layer near the surface (Eq. 8).

$$\beta = 7.7\ 10^{-9} h_c \tag{8}$$

However, since the existing empirical formulae for the CHTC as a function of wind speed are based on only a limited number of measurements at a few facade positions and for a few building configurations, and more detailed information is not available, HAM models use Eq. (5) at all facade positions. Therefore, more research is needed. Wind tunnel and especially full-scale measurements are expensive and time-consuming. CFD can provide a suitable alternative, but the accuracy of CFD is an issue of concern and careful application and model validation are imperative.

This paper presents high-resolution CFD simulations of forced convective heat transfer at the facades of a low-rise cubic building (10x10x10m³). The objectives are: (1) to analyse the distribution of CHTC across the facades; (2) to investigate the correlation between CHTC and local wind speed across the windward facade; (3) to analyse the thickness of the laminar sublayer dominating boundary layer heat transfer; (4) to assess the impact of high-resolution versus low-resolution grids on the accuracy of CTHC simulations; and (5) to briefly address the relationship between CHTC and wind-driven rain (WDR) distributions across the facade. In section 2, two near-wall modelling approaches are briefly outlined. In section 3, CFD model validation is performed. Section 4 describes the application of the model for forced exterior convective heat transfer. The results are reported in section 5. Sections 6 present discussion and conclusions.

2. Wall functions versus low-Reynolds number modelling

In CFD simulations, generally, two options exist for modelling near-wall turbulence: wall functions or low-Reynolds number modelling. They differ in the way in which the boundary layer at wall surfaces is taken into account. This boundary layer consists of an inner layer, including the thin laminar sublayer, the buffer layer and the logarithmic layer, and a fully turbulent outer layer. Low-Re number modelling refers to resolving the whole boundary layer by placing control volumes in each part of the boundary layer. Because the thickness of the laminar sublayer is inversely proportional to the flow Re number and Re numbers for wind flow around buildings are quite large, the laminar sublayer is often very thin and a high to very high grid resolution is required close to the walls. Because of the computational cost associated with low-Re number modelling, wall functions are often used instead. They are semi-empirical formulae that bridge the region between the wall and the logarithmic layer, and provide an approximation of the effect of the wall on the mean wind speed and turbulence quantities in the logarithmic layer. Much coarser grids can be used here. This is schematically depicted in Fig. 1. The grid resolution at a wall boundary is characterised by the dimensionless wall distance $y^+ = u^* y_P / \nu$, where u^* is the friction velocity, y_P the distance from the centre point P of the wall-adjacent cell to the wall and ν the kinematic viscosity. Appropriate grids for low-Re number modelling have a y^+ below 5 (and about equal to 1) to ensure that the centre point P of the wall-adjacent cell is situated in the laminar sublayer. Wall functions grid should have a y^+ above 30 and below 500 to ensure that P is situated in the logarithmic layer.

3. Model validation

CFD simulations based on the steady-state Reynolds-averaged Navier-Stokes (RANS) equations in combination with a turbulence model require model validation, i.e. the comparison of simulation resuls with accurate experimental data that is relevant for the situation under study. Due to lack of available experimental data of CHTC at realistic Reynolds numbers for building applications (Re ~ 10^5-10^6), validation is performed based on wind tunnel measurements of the velocity field very close to the windward surface of a cubic building with dimensions 0.2x0.2x0.2 m³ (Minson et al. 1995). The CFD simulations are performed at wind tunnel scale. The building model is placed in a computational domain of length x width x height = 4.2 x 4.2 x 2 m³. The domain is discretised by a hybrid grid with about 1.5×10^6 cells, with the centre of the smallest cell being at a distance y_P = 160 μm from the building surface. While this very high resolution is strictly not necessary for the velocity simulations, it is very important for the heat transfer simulations that will be performed with low-Re number modelling in the next section.

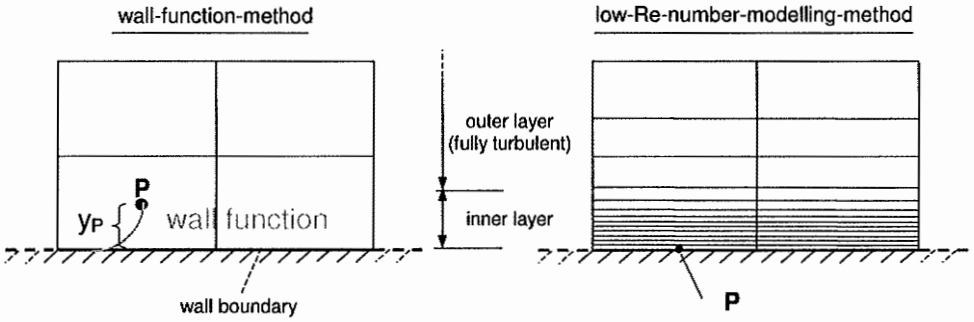

FIG. 1: Schematic representation of part of a grid with control volumes near a wall boundary. Left: wall function grid. Right: low-Re number modelling grid. P denotes the centre point of the wall-adjacent cell.

The inlet mean wind speed and turbulence profiles are taken equal to the measured wind tunnel profiles. Because low-Re number modelling in Fluent 6.3 is employed, no roughness can be assigned to the bottom of the computational domain and it is treated as a zero-roughness no-slip boundary. This will inevitably give rise to unintended streamwise gradients (horizontal inhomogeneity; Blocken et al. 2007). To limit these gradients, the distance between the inlet plane and the windward facade of the building model is limited to 5H (H = 10 m). At the outlet of the domain, zero static pressure is specified. The sides and the top of the domain are modelled as slip walls (zero normal velocity and zero normal gradients of all variables).

Steady-state, isothermal, 3D RANS simulations are made using the high-Reynolds number realizable k-ε model (Shih et al. 1995) in combination with the low-Reynolds number Wolfhstein model (Wolfhstein 1969). Except for a very thin region at the top edge of the building, y^+ values are below 1 across all facades with the present grid and with the reference wind speed U_{10} = 3 m/s. Pressure-velocity coupling is taken care of by the SIMPLE algorithm. Pressure interpolation is second order. Second order discretization schemes are used for both convection terms and viscous terms of the governing equations.

The results are presented as ratios of the streamwise (U) and vertical (V) wind speed to the reference wind speed U_{10} at building height, along a set of vertical lines in the cube centreplane (Figs. 2 and 3). A fair to good agreement is obtained. The agreement is less good for the frontal vortex region upstream of the cube (shown in Fig. 4), but very good for the upper part (y/H > 0.4) close to the cube. The discrepancies are attributed to the well-known stagnation point anomaly of the k-ε models (Franke et al. 2007). A better agreement would have been obtained with Reynolds stress models, however convergence with such models could not be obtained with steady-state simulations on the high-resolution and high-gradient grid used in this study. Regardless, the performance of steady-state RANS with the realizable k-ε is considered sufficient for the purposes of this paper. Note however that larger discrepancies than shown in Fig. 3 will occur for wind speed downstream of the windward facade and for other wind directions because of the limitations of the realizable k-ε model.

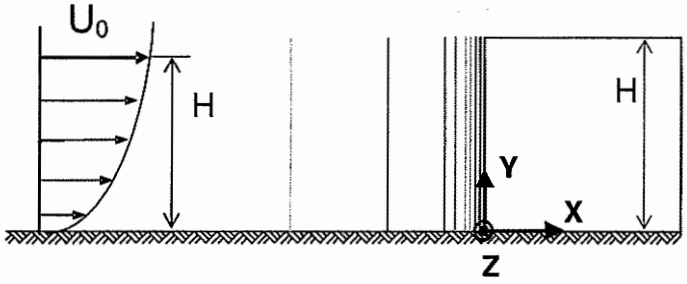

FIG. 2: Vertical lines in the cube centreplane along which wind speed ratios are presented in Fig. 3.

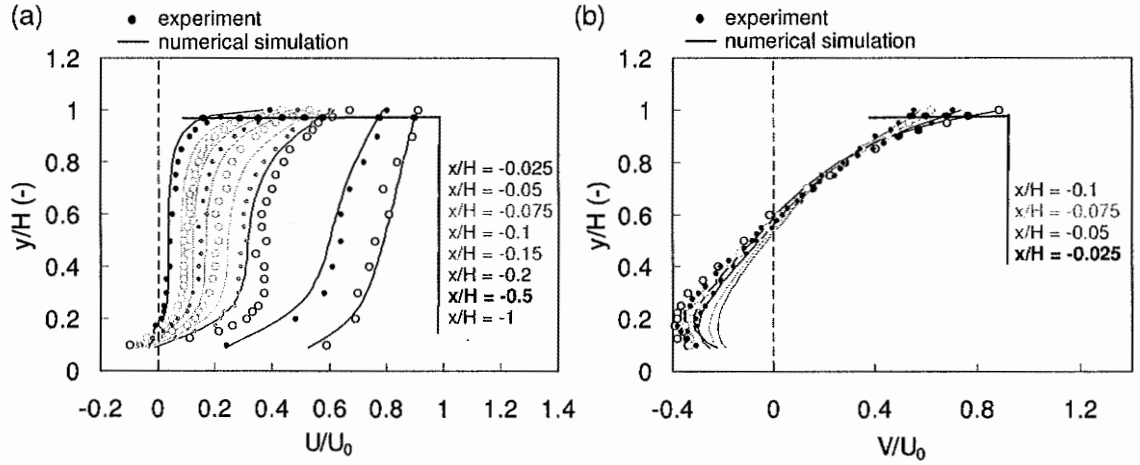

FIG. 3: Numerical and experimental results for the wind speed ratios U/U_0 and V/U_0 along the vertical lines shown in Fig. 2.

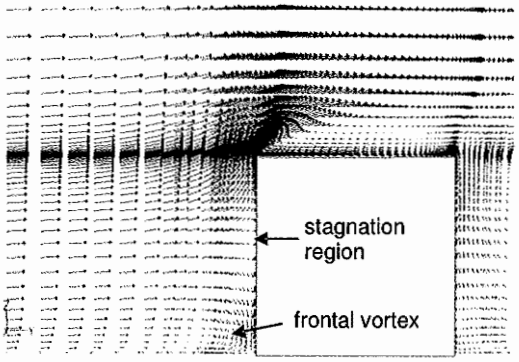

FIG. 4: Velocity vectors in the vertical cube centreplane with indication of stagnation region and frontal vortex.

4. Model application for forced convective heat transfer

The geometrical model, the computational domain and the computational grid are scaled up to full scale (10 m cubic building). Steady-state simulations with the RANS approach and the realizable k-ε model are conducted. The low-Re number Wolfhstein model, as well as standard and non-equilibrium wall functions will be used. These thermal simulations are performed with a fixed building surface temperature of 303 K and an inlet air temperature of 283 K. The bottom wall of the computational domain is adiabatic. The reference temperature to determine the CHTC is the inlet temperature (283 K). Only forced convection is taken into account. This situation is physically only valid for high wind speed. The threshold reference wind speed value for which forced convection eliminates buoyancy effects is not known and is the subject of future research.

The simulations are performed with typical atmospheric boundary layer wind speed profiles over a grass-covered terrain with aerodynamic roughness length $y_0 = 0.03$ m. The reference wind speed at building height $U_{10} = 3$ m/s. The turbulence intensity ranges from 20% at ground level to 5% at gradient height. Turbulent kinetic energy is calculated based on turbulence intensity ($k = \frac{1}{2}(\sigma_u^2 + \sigma_v^2 + \sigma_w^2) \approx (I_u U)^2$) and turbulence dissipation rate $\varepsilon = u^{*3}/\kappa(y+y_0)$ where u^* is the friction velocity, κ the von Karman constant (~ 0.42) and y the height co-ordinate. CFD simulations are performed for wind directions perpendicular to the windward facade ($\theta = 0°$) and for oblique wind ($\theta = 22.5°$, 45° and 67.5°). The results are presented in the next section.

5. Results

5.1 CHTC distribution across the facade

The ratio of CHTC to reference wind speed (h_c/U_{10}) is shown along the perimeter of a vertical and a horizontal cross-section of a plane midway through the building (Fig. 5). Results are given for $\theta = 0°$ and $\theta = 45°$. High gradients exist across the facade, with maximum values at the windward top and vertical edges.

5.2 Correlation between CHTC and local wind speed

Fig. 5 has shown that the CHTC reaches its highest values at positions where also the local wind speed is high, i.e. near the top edge and the vertical side edges of the windward building facade(s). This might suggest that there is a strong correlation between CHTC and the local wind speed $V_{3D,loc}$ or $V_{2D,loc}$ taken at a certain distance from the facade. $V_{2D,loc}$ refers to the magnitude of the wind velocity vector parallel to the facade. For each separate point at the building facade, the correlation between CHTC and $V_{2D,loc}$ is indeed present, as demonstrated by the full-scale measurements by Sharples (1984) and as confirmed by the present simulations. Note that changing $V_{2D,loc}$ for $V_{3D,loc}$ has no significant influence on the correlations. However, it might also be suggested that the relationship between both parameters is similar across the facade. In other words, that CHTC and $V_{2D,loc}$ are spatially correlated, and that this correlation will be stronger when $V_{2D,loc}$ is taken closer to the facade. Figs. 6a-c show the correlation for the windward facade, for $\theta = 0°$ and for $V_{2D,loc}$ taken in the laminar sublayer/buffer layer (d = 0.001 m) and at a distance of 0.1 and 0.3 m from the facade. The correlation is not significant, which is not surprising given the presence of heat fluxes across the facade in the boundary layer. Fig. 6d shows that a stronger correlation exists between CHTC and the turbulent kinetic energy for d = 0.001 m, indicating the importance of turbulent fluctuations in the wind velocity pattern on surface heat transfer.

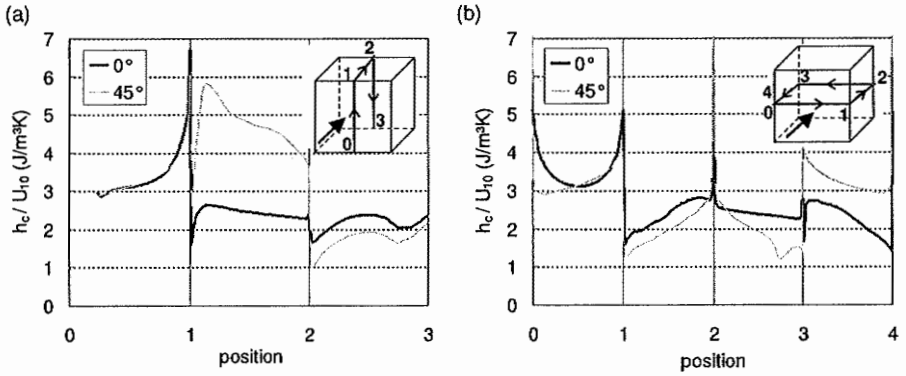

FIG. 5: Ratio of CHTC to reference wind speed U_{10} along lines on the cubic building surfaces, for wind direction $\theta = 0°$ and $\theta = 45°$.

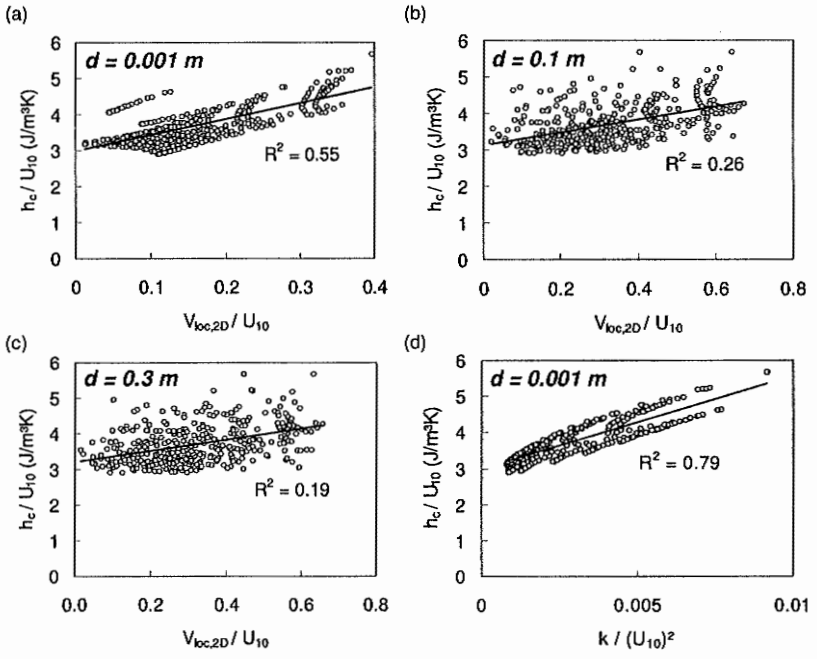

FIG. 6: (a-c) Correlation between the ratios h_c/U_{10} and $V_{loc,2D}/U_{10}$ for positions at different distances from the windward facade ($\theta = 0°$). (d) Correlation between h_c/U_{10} and $k/(U_{10})^2$.

5.3 Thickness of the laminar sublayer

As mentioned earlier in section 2, low-Reynolds number modelling requires grids where the first cell is situated in the laminar sublayer ($y_P < d_{lam}$). This requirement is similar to the requirement $y^+ < 5$. However, to the knowledge of the authors, there is no information in literature on the thickness of the laminar sublayer (d_{lam}) at building surfaces. In addition, y^+ values for a certain grid and simulation can only be obtained after a simulation has been performed, because the value of u* that is required to calculate y^+ is not known a priori. Therefore, an iterative procedure is required. First, the required y_P value is estimated, then the simulation is performed, and after the y^+ values are checked. Based on these values, the grid is refined or coarsened, after which the simulation is repeated on the adapted grid. For future simulations, information on d_{lam} can be useful to provide a better initial guess for y_P and/or to avoid this iterative procedure. In this study, d_{lam} for the windward facade, for $U_{10} = 3$ m/s and for $\theta = 0°$ was calculated based on the obtained y^+ values, using the knowledge that the laminar sublayer ends to about $y^+ = 5$. Fig. 7 shows the distribution of d_{lam} along the two cross-section perimeters. Note that U_{10} and d_{lam} are inversely proportional. Fig. 7 indicates that the present grid (with $y_P = 160$ μm) includes several cells in the laminar sublayer.

5.4 Wall functions versus low-Re number modelling

Previous CFD simulations of exterior forced CHTC for buildings were made using wall functions (Emmel et al. 2007). Wall functions allow avoiding high-resolution computational grids and performing faster and computationally less expensive simulations. However, wall functions are based on certain assumptions. The standard wall functions by Launder and Spalding (1974) assume local boundary layer equilibrium, which is certainly not a valid assumption for the complex flow around buildings. The non-equilibrium wall functions by Kim and Choudhury (1995) take into account effects of pressure gradients and strong non-equilibrium. However, both types of wall functions do not take into account the specifics of flow in the laminar sublayer. Because heat transfer in this layer occurs mainly by conduction, it determines to a large extent the CHTC. Therefore, accurate simulations of CHTC in complex flow patterns can generally not be obtained with wall functions. Instead, low-Reynolds number modelling on high-resolution grids is required. To demonstrate this, simulations have also been made with a low-resolution wall function grid ($y^+ > 30$). Both standard wall functions and non-equilibrium wall functions have been used. Fig. 8 indicates that the use of wall functions significantly overestimates the CHTC at almost all positions along the two perimeters. As expected, standard wall functions perform worse than non-equilibrium wall functions.

5.5 CHTC and wind-driven rain

Fig. 9 compares the spatial distribution of the ratio CHTC to U_{10} and the catch ratio (WDR rain intensity divided by reference horizontal rainfall intensity R_h), both for the same building and for wind direction $\theta = 0°$. Note that the data below the dashed line in Fig. 9a is unreliable due to grid resolution issues near the bottom of the computational domain (Blocken et al. 2007). Fig. 9 shows a strong similarity between both spatial distributions. This implies that also the CVTC will be higher at this location and that the facade parts that receive most WDR also experience most intensive drying.

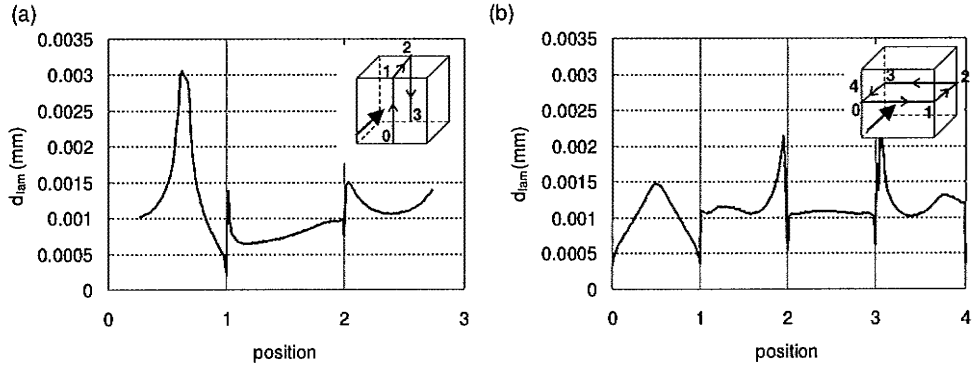

FIG. 7: Thickness of the laminar sublayer d_{lam} along the perimeter of a vertical and horizontal cross-section.

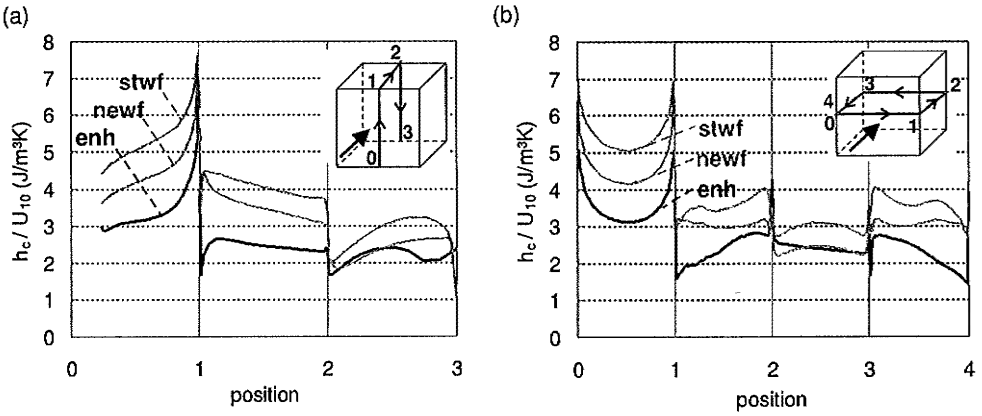

FIG. 8: CFD simulation results for the ratio of h_c/U_{10} as obtained with low-Reynolds number modelling ("enh") and with standard ("stwf") and non-equilibrium wall functions ("newf").

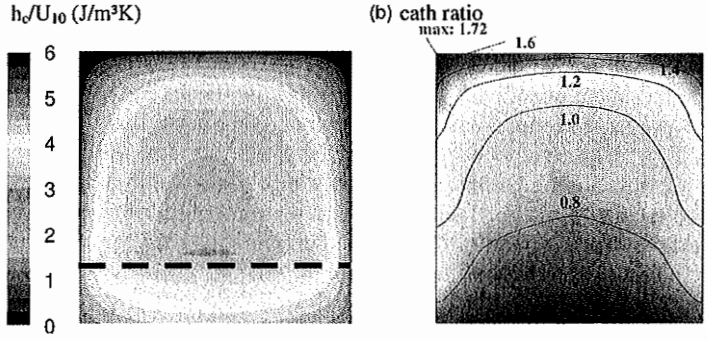

FIG. 9: (a)Distribution of h_c/U_{10} across the windward facade (for U_{10} = 3 m/s, θ = 0°); (b) Distribution of the WDR catch ratio across the same windward facade (for U_{10} = 10 m/s, R_h = 1 mm/h, θ = 0°).

6. Discussion and conclusions

This study was based on the steady-state RANS approach in combination with the realizable k-ε model and the Wolfhstein model. These models are less appropriate for solving wind flow around buildings downstream of the plane in which the windward facade is situated, because in this downstream region transient features, separation and recirculation dominate the flow. Therefore, this paper has mainly focused on the windward facade. Future and ongoing research includes transient simulations on high-resolution grids (Defraeye et al. 2008).

The conclusions of this study are: (1) wind flow around the building introduces a very distinct CHTC distribution across the facade; (2) no significant correlation exists between the CHTC and the local wind speed *across* the facade; (3) the laminar sublayer for the building and conditions in this paper has a thickness of about 1 mm; (4) standard and non-equilibrium wall functions are not able to capture the complexity of wind-induced heat transfer, therefore low-Re number modelling on high-resolution grids is imperative; (5) the CHTC distribution across the windward facade shows some similarity to the distribution of wind-driven rain (WDR), with both parameters reaching high levels near the top edge of the facade. This implies that also the convective vapour transfer coefficient will be higher at this location and that the facade parts that receive most WDR also experience most intensive drying.

7. References

ASHRAE (1975). ASHRAE Task Group. Procedure for determining heating and cooling loads for computerising energy calculations. Algorithms for building heat transfer subroutines. New York.

Blocken B, Stathopoulos T, Carmeliet J. (2007). CFD simulation of the atmospheric boundary layer: wall function problems. Atmospheric Environment 41(2): 238-252.

CIBS. 1979. Chartered Institute of Building Services Guide Book A, Section A3. London.

Defraeye T, Blocken B, Carmeliet J. (2008). Analysis of the the exterior convective heat transfer coefficients of a cubic building with CFD. This symposium.

Franke J, Hellsten A, Schlünzen H, Carissimo B. (2007). Best practice guideline for the CFD simulation of flows in the urban environment. COST Action 732: Quality Assurance and Improvement of Microscale Meteorological Models.

Ito N, Kimura K, Oka J. (1972). A field experiment study on the convective heat transfer coefficient on exterior surface of a building. ASHRAE Trans. 78: 184-191.

Jürges W. (1924). Der Wärmeübergang an einer ebenen Wand. Beizh. z. Gesundh. Ing. 1(19)

Kim SE, Choudhury D. (1995). A near-wall treatment using wall functions sensitized to pressure gradient", ASME FED Vol. 217, Separated and Complex Flows.

Launder BE, Spalding DB. (1974). The numerical computation of turbulent flows. Comput. Method. Appl. M. 3: 269-289

Minson AJ, Wood CJ, Belcher RE. (1995). Experimental velocity measurements for CFD validation. Journal of Wind Engineering and Industrial Aerodynamics 58: 205-215

Sharples S. (1984). Full scale measurements of convective energy losses from exterior building surfaces. Building and Environment 19: 31-39.

Shih TH, Liou WW, Shabbir A, Zhu J. (1995). A new k-ε eddy-viscosity model for high Reynolds number turbulent flows – model development and validation. Computers and Fluids 24 (3): 227-238

Wolfstein M. (1969). The velocity and temperature distribution of one-dimensional flow with turbulence augmentation and pressure gradient. International Journal of Heat and Mass Transfer 12: 301-318.